Cut-and-Pasting Ligands: The Structure/Function Relationships of a Thermally Robust Mo(VI) Precursor

Michael A. Land,[a] *Dexter A. Dimova,*[a] *Katherine N. Robertson,*[b] *and Seán T. Barry* [a]

[a] Department of Chemistry, Carleton University, 1125 Colonel By Drive, Ottawa, Ontario, K1S 5B6 Canada

[b] Department of Chemistry, Saint Mary's University, 923 Robie Street, Halifax, Nova Scotia, B3H 3C3 Canada

Keywords: Precursor Design, Volatility, Thermal Stability, Chemical Structure, Molybdenum

Abstract

The bis(*tert*-butylimido)-molybdenum(VI) framework has previously been used for the successful atomic layer deposition and chemical vapor deposition of many molybdenum-containing thin films. We have now prepared and fully characterized a new thermally robust bis(*tert*-butylimido)molybdenum(VI) complex, bis(*tert*-butylimido)-bis(*N*-2-(*tert*-butyliminomethyl)pyrrolato)-molybdenum(VI), $(^tBuN)_2Mo(PyrIm)_2$ (**1**), that incorporates two *N,N'-*κ_2-monoanionic ligands. The volatility and thermal stability of **1** was measured using thermogravimetric analysis and differential scanning calorimetry, where it was found to achieve a 1 Torr of vapor pressure at 212 ºC and had an onset of thermal decomposition at 273 ºC. Comparison of its thermal properties to the known ALD precursor $(^tBuN)_2Mo(dpamd)_2$ (dpamd = *N,N'*-diisopropyl-acetamidinato) showed that **1** exhibits a similar volatility, but with a 78 ºC improvement in thermal stability. Since **1** exhibits an excellent thermal range (61 ºC), it should be further explored for use as a vapor deposition precursor.

Introduction

Molybdenum-containing thin films are very versatile, having found applications in microelectronic manufacturing,[1] high-surface area heterogeneous catalysis,[2] gas-sensing,[3] optical materials,[4] and lubricants,[5] to name a few. One common method used to prepare Mo-containing thin films, with sub-nanometer thickness control, is atomic layer deposition (ALD). ALD relies on chemical precursors that are delivered in the vapor phase to a substrate, where they subsequently undergo gas-surface reactions and chemisorb. Then, in conjunction with a co-reagent, they react in a stepwise fashion to deposit thin films. The most important criteria in the design of potential precursors are thermal stability, volatility, and surface reactivity.[6] While volatility and surface reactivity are both important for the deposition of thin films, this manuscript will focus on the thermal stability of the chemical precursors. In particular, these compounds must have adequate thermal stability in a precursor delivery vessel during deposition to ensure consistent gas phase pressure and composition.

A common molecular scaffold used in the syntheses of volatile molybdenum precursors is the bis(*tert*-butylimido)-molybdenum(VI) framework. For example, the bis(*tert*-butylimido)-molybdenum(VI) framework incorporating anionic *N,N'*-chelating ligands has previously been used for the ALD and CVD of various molybdenum-containing films. The amidinate **2** has been used in conjunction with O_3 for the ALD of MoO_3.[3] It has also been employed for the CVD of MoN_x[7,8] and MoS_2,[9] using NH_3 and S_8 as co-reagents, respectively. Additionally, MoN_x nanoparticles have been prepared from the thermolysis of the pyrazolate **A**.[10] Dianionic *N,N'*-chelating ligands have also been used to prepare volatile molybdenum compounds; for example, the diazabutadienyl **B** has been used for the CVD of MoS_2 using S_8 as a co-reagent.[11] A similar molybdenum compound that contains only one monoanionic *N,N'*-chelating ligand, the guanidinate **C**, generated MoC_xN_y in the presence of NH_3, by CVD and has also been used as a single-source precursor for the CVD of Mo_2C.[12]

Other similar compounds not used for ALD or CVD, but of structural importance to this work, are listed in Chart 1 as well. For example, the synthesis of the amidinate **2** can be stopped after the addition of just one ligand, to form the amidinate mono-chloride **D**, which is a sublimable solid (170 ºC, 225 mTorr).[13] The preparation of the hydrazido **E**, a

distillable oil (75 ºC, 0.75 mTorr) also stops at the mono-chloride, likely due to the steric congestion from two *tert*-butylimido ligands, whereas bis-addition of the hydrazido ligand was achieved for the less bulky Group 5 analogues, (^{t}BuN)MCl$_3$ (M = Nb, Ta).[14]

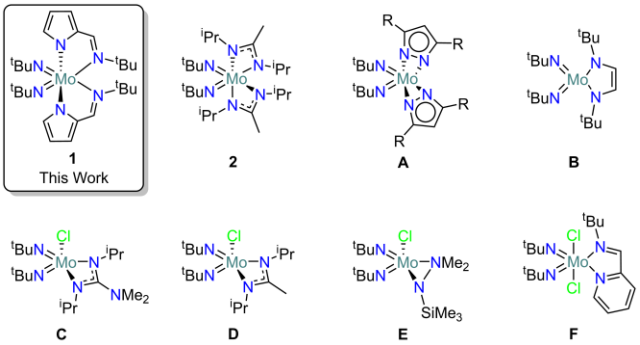

Chart 1. Known vapor deposition precursors, or volatile compounds, containing the bis(*tert*-butylimido)molybdenum(VI) framework. ^{t}Bu = *tert*-butyl; ^{i}Pr = isopropyl; Me = methyl; R = ^{t}Bu or phenyl.

We have recently prepared a series of (^{t}BuN)$_2$MoCl$_2$·L (L = neutral *N,N'*-chelating ligand) compounds and reported their volatilities and thermal stabilities.[15] Additionally, we examined their mechanism of decomposition and found that they decompose *via* γ-H activation of the *tert*-butylimido group. This first yields isobutene and (^{t}BuNH)MoNCl$_2$, the latter of which subsequently decomposes to give *tert*-butylamine and MoN$_x$.[16] It has previously been shown that (^{t}BuN)$_2$MoCl$_2$·2py is a single-source precursor for the CVD of MoC$_x$N$_y$, with no Cl contamination.[17] Additionally, the use of chloride-containing compounds can be exploited for the deposition of chlorine-free metal films,[18] although halogens are generally avoided in precursor design as the byproducts can etch the growing film or damage a metal reactor. One way to remove chloride ligands during precursor design is through salt metathesis reactions with an alkali salt of an anionic ligand. Additionally, ligation (with anionic or neutral ligands) can also be used to tune the volatility, thermal stability, and chemical reactivity of metal complexes.

In our recent study we found that by using unsymmetric ligands we could combine the thermal stability of an aromatic heterocycle with the volatility conferred from the presence of a *tert*-butyl imino moiety.[15] For example, the imino-pyridine ligand (impy, **F**, Chart 1), integrates the superior thermal stability of the 2,2'-bipyridine ligand with the

excellent volatility of the 1,4-di-*tert*-butyl-1,3-diazabutadiene ligand.[15] Herein, we describe application of the same method to anionic ligands, for the preparation of a volatile, yet thermally stable, molybdenum precursor. We have synthesized and characterized a molybdenum compound that incorporates the *N*-2-(*tert*-butyliminomethyl)pyrrolate (PyrIm) ligand, which combines an aromatic heterocyclic with a pendant *tert*-butylimino moiety.

Results and Discussion

Synthesis and Characterization

We first prepared the known bis(*tert*-butylimido)-dichloromolybdenum(VI) 1,2-dimethoxyethane (dme) adduct, (^{t}BuN)$_2$MoCl$_2$·dme, as our Mo(VI) starting material.[19] Treatment of (^{t}BuN)$_2$MoCl$_2$·dme with two equivalents of both sodium hydride and *N*-2-(tert-butyliminomethyl)pyrrole (HPyrIm)[20] immediately resulted in a reddish-orange mixture (Scheme 1). After filtration and purification by crystallization, bis(*tert*-butylimido)-bis(*N*-2-(*tert*-butyliminomethyl)pyrrolato)-molybdenum(VI), (^{t}BuN)$_2$Mo(PyrIm)$_2$ (**1**), was isolated in moderate yield, as red, block-shaped crystals.

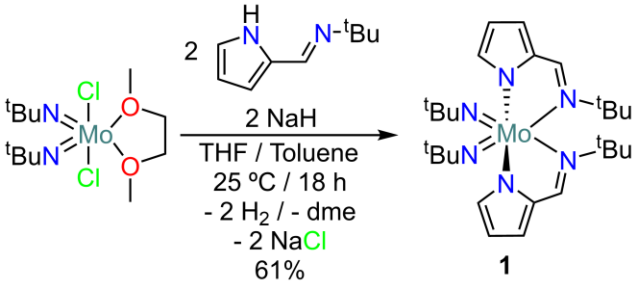

Scheme 1: Synthesis of (^{t}BuN)$_2$Mo(PyrIm)$_2$ (**1**).

The ^{1}H and ^{13}C NMR spectra confirmed the structure of **1**, with both showing two equivalent PyrIm environments. Combined with spectral evidence of two equivalent *tert*-butylimido ligands, the octahedral complex **1** must adopt a *cis* geometry, and this was confirmed using single-crystal X-ray diffraction (vide infra). The ^{1}H NMR spectrum of **1** showed slight deshielding of the pyrrole ring in the anionic PyrIm ligand, compared to its ligand precursor (HPyrIm). In contrast, the *tert*-butylimino moiety was slightly shielded

(compared to HPyrIm) suggesting delocalization throughout the entire ligand framework. Thus, the imino group cannot just be a spectator moiety forming a dative bond to Mo. The ^{15}N NMR spectrum of **1** had three nitrogen environments and their chemical shifts were consistent with similar Mo compounds.[21,22] Finally, the bulk composition of **1** was verified using EA and the molecular ion corresponding to **1** was detected using EI-HRMS; an analysis of the fragmentation of **1** can be found in the SI.

Finally, we attempted to prepare other bis(*tert*-butylimido)-molybdenum(VI) compounds that contain two monoanionic *N,N'*-chelates. The ligands chosen were *N,N*-dimethyl-*N',N''*-diisopropyl-guanidinate (^{iPr}gaun) and *N,N'*-dimethyl-pentane-2,4-diimidate (^{Me}nacnac);[23] however neither resulted in the isolation of bis-addition products of the ligand. The reaction between (^{t}BuN)$_2$MoCl$_2$·dme and Li[^{iPr}guan] resulted in the known adduct **C** (Chart 1);[24] the crystal structure of which was hitherto unknown. Additionally, the reaction between (^{t}BuN)$_2$MoCl$_2$·dme and Li[^{Me}nacnac] resulted in an intractable mixture, however, a single-crystal of (^{t}BuN)$_2$MoCl(^{Me}nacnac) was isolated from this mixture and its structure is described in the SI.

X-Ray Crystallography

The results from the single-crystal X-ray diffraction studies of *N*-2-(*tert*-butyliminomethyl)pyrrole (HPyrIm), and the bis(*tert*-butylimido)molybdenum(VI) adduct that incorporates it, (^{t}BuN)$_2$Mo(PyrIm)$_2$ (**1**), are reported herein. Additionally, we report the crystal structures of (^{t}BuN)$_2$MoCl(^{iPr}guan) and (^{t}BuN)$_2$MoCl(^{Me}nacnac) in the supporting information. Additional crystallographic parameters and images can also be found in the supporting information.

The ligand precursor, *N*-2-(*tert*-butyliminomethyl)pyrrole (HPyrIm), was found to crystallize in the monoclinic $P2_1/n$ space group as colorless blocks (Figure 1). The asymmetric unit is comprised of two unique molecules that are held together by N−H…N hydrogen-bonds (N1−H1n…N4 = 2.078(12) Å, N3−H3n…N2 = 2.102(13) Å). The two HPyrIm molecules that comprise the dimer have an angle of 79.96(3)º between the planes, defined by each pyrrole ring. The C−C and N−C bond lengths of the pyrrole ring are not exactly as expected for alternating double and single bonds, instead each are intermediate with the ring forming an aromatic heterocycle (Table 1). As expected, the bond length in the imine moiety of HPyrIm (N2−C5) is indicative of double bond character,

and the C4−C5 bond of the ligand backbone is single (Table 1). The average bond lengths of HPyrIm are consistent with those reported previously for other *N*-2-(iminomethyl)pyrroles.[25] Finally, other than the hydrogen bonds described above, there are not any notable intermolecular interactions between different molecules in the asymmetric unit.

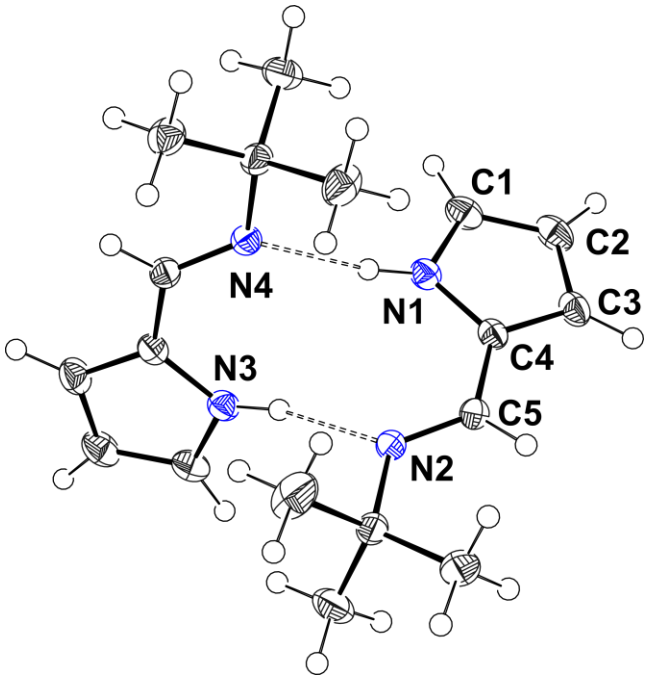

Figure 1. Solid-state structure of *N*-2-(*tert*-butyliminomethyl)pyrrole (HPyrIm); two molecules are held together in a dimer via N−H…N hydrogen bonds (dashed lines). Thermal ellipsoids are drawn at the 50% probability level.

Table 1. Selected bond lengths of the neutral ligand precursor (HPyrIm) and the adduct that incorporates it as an anionic ligand, (^{t}BuN)$_2$Mo(PyrIm)$_2$ (**1**).[a]

Compound	C1−C2 / Å	C3−C4 / Å	C4−C5 / Å	N2−C5 / Å	N1−C4 / Å
HPyrIm	1.3767(12) 1.3758(12)	1.3846(9) 1.3848(10)	1.4456(10) 1.4434(10)	1.2754(9) 1.2769(9)	1.3700(9) 1.3720(9)
1	1.368(8) 1.382(14)	1.385(8) 1.404(13)	1.419(8) 1.382(13)	1.316(7) 1.281(12)	1.369(7) 1.34(9)

[a] The second value listed for each compound corresponds to the analogous bonds in the second HPyrIm molecule comprising (N3, N4, C10−C18) and to the first component of the disordered ring in model **1**, respectively.

In the solid-state structure of (^{t}BuN)$_2$Mo(PyrIm)$_2$ (**1**), the molybdenum center has an octahedral coordination environment (Figure 2). One of the PyrIm ligands (comprising N3 and N4) is disordered over two positions, with the *tert*-butylimino moiety (of the PyrIm ligand) and the *tert*-butylimido ligand (N5) occupying the same positions (see SI). In line with all reported Group 6 bis(imido) complexes,[25] the *tert*-butylimido ligands in **1** are *cis* to each other. The pyrrole rings are *trans* to each other and the *tert*-butylimino groups of the PyrIm ligand are *trans* to each *tert*-butylimido ligand. Therefore, the octahedral complex **1** is best described as a (*Λ*)-*cis*-[(^{t}BuN)$_2$Mo(PyrIm)$_2$] complex. The average Mo−N(imido) bond lengths in **1** (1.774(7) and 1.818(13) Å) are longer than the corresponding bonds in the (^{t}BuN)$_2$MoCl$_2$·L (L = neutral *N,N'*-chelate) compounds we have recently reported (average: 1.739(5) Å).[15] The PyrIm ligands are quite electron-rich, therefore a smaller contribution from the *tert*-butylimido ligands is required to satisfy the molybdenum center.

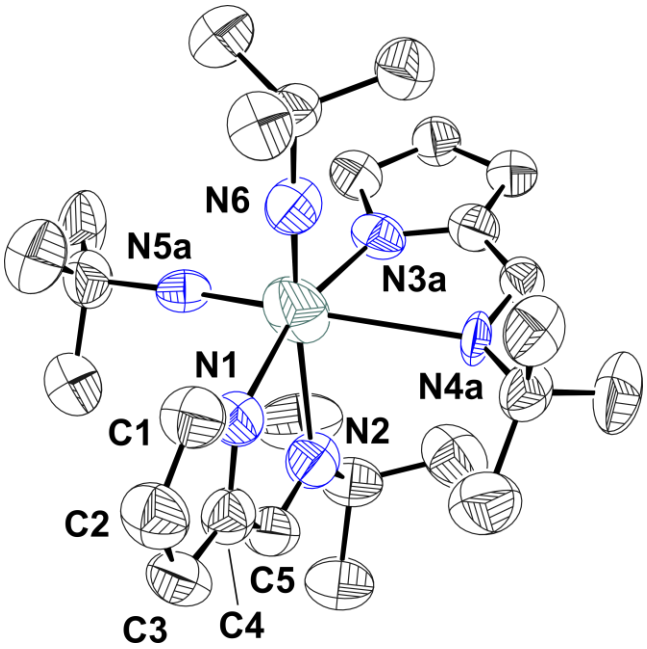

Figure 2. Solid-state structure of (^{t}BuN)$_2$Mo(PyrIm)$_2$ (**1**). Thermal ellipsoids are drawn at the 50% probability level. Hydrogen atoms have been omitted for visual clarity. The PyrIm

ligand (comprising N3 and N4) and the imido ligand (comprising N5) are disordered over two positions (see the SI); however, only part A of the disorder is shown.

The bond lengths in the pyrrole ring of the PyrIm ligand in **1** show slight deviations compared to those in the ligand precursor (Table 1). Most notable are the elongation of the imino bond (N2−C5) and the shortening of the C4−C5 bond of the ligand backbone (Table 1). This suggests that there is significant delocalization in the anionic ligand framework, specifically in the imino backbone, upon ligation. It must contribute electronically to the stabilization of the complex, rather than just forming a dative bond to the metal center. Despite being relevant for vapor phase depositions, **1** is only the second structurally characterized bis(*tert*-butylimido)molybdenum(VI) complex that incorporates two *N,N*'-chelating ligands, the other being $(^{t}BuN)_2Mo(Pz)_2$ (Pz = 3,5-di-*tert*-butylpyrazolato) (**A**).[26] Finally, **1** does not form any intermolecular interactions below the sum of the Van der Waals radii. There are only a few long-range, weak C−H…H interactions between molecules, a feature which certainly contributes to the observed volatility of **1** (vide infra).

Volatility and Thermal Stability

$(^{t}BuN)_2Mo(PyrIm)_2$ **1** was investigated to determine if it would be a suitable precursor for the deposition of molybdenum-containing films. Thermogravimetric analysis (TGA) of **1** showed a single-step mass loss curve, with an onset of volatilization of 188 ºC (Figure 3a). Additionally, **1** completely evaporated before 300 ºC without decomposition, as indicated by a residual mass of 0%. Isothermal TGA of **1** showed a single-step mass loss, with complete evaporation at selected isotherms between 190 and 250 ºC. The rates of evaporation ranged between 60 and 900 $\mu g \cdot min^{-1} \cdot cm^{-2}$, with respect to the two boundary temperatures, at atmospheric pressure (Figure 3b).

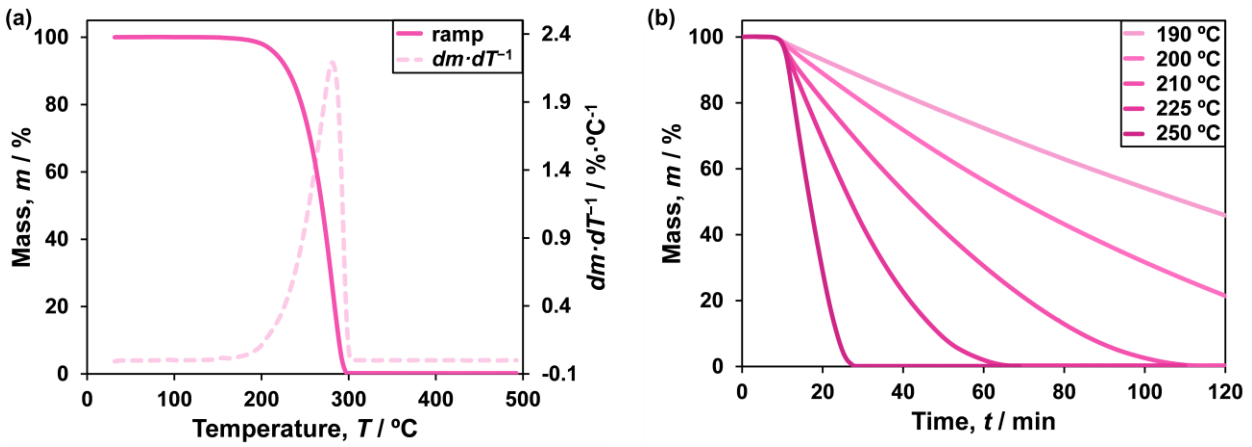

Figure 3. (a) Thermogravimetric analysis of (^{t}BuN)$_2$Mo(PyrIm)$_2$ (**1**), with a heating rate of 10 ºC·min^{-1}. The mass loading was 10.1 mg and the residual mass was 0.2%. (b) Isothermal thermogravimetric analysis of **1**. The samples were heated at 20 ºC·min^{-1} and then were held at the designated isothermal temperature. The mass loadings were 10.0 ± 0.1 mg for each sample.

To further quantify the volatility of (^{t}BuN)$_2$Mo(PyrIm)$_2$ **1** its vapor pressure was estimated using a previously reported model, which uses the first derivative of the mass loss curve.[27,28] Using this model the temperature at which a precursor achieves 1 Torr of vapor pressure (T_V), a commonly desired pressure for ALD and CVD precursors in industrial deposition tools, can be determined. The T_V for **1** was estimated to be 212 ºC, which is high for an ALD process temperature (Figure 4), so it was compared to a previously used deposition precursor, (^{t}BuN)$_2$Mo(dpamd)$_2$ (**2**).[3,7–9] Compound **2** was prepared following reported methods[7] before thermogravimetric analysis was carried out (Figure S31), for direct comparison to **1**. The T_V for **2** was estimated to be 206 ºC, which is nearly identical to that of **1** (Figure 4).

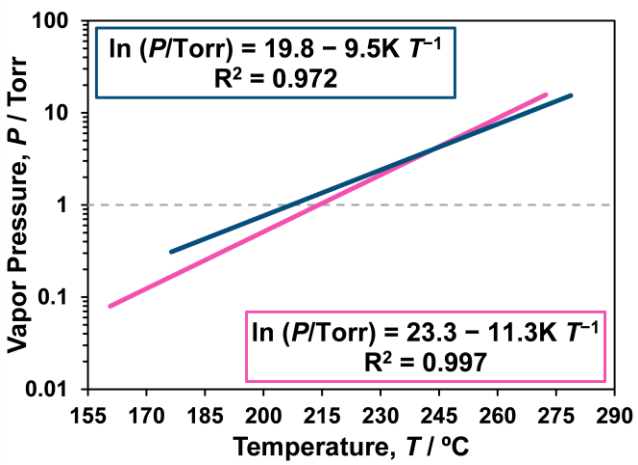

Figure 4. Vapor pressure of (^{t}BuN)$_2$Mo(PyrIm)$_2$ (**1**) (pink, bottom) and (^{t}BuN)$_2$Mo(dpamd)$_2$ (**2**) (blue, top) modeled according to the Langmuir equation estimated from TGA.[27,28] A horizontal line is drawn at 1 Torr of vapor pressure (T_V at 212 ºC for **1** and 206 ºC for **2**).

Despite having a high T_V, it has been shown that **2** can be delivered into ALD or CVD reactors between the temperatures of 80-145 ºC.[3,7–9] These lower delivery temperatures are viable because of the fast kinetics for the vaporization of the precursor. A sublimation experiment was performed on **1**, which showed that it sublimed without decomposition at 150 ºC (40 mTorr), akin to **2**. Because **1** and **2** have similar volatilities, it is possible that (^{t}BuN)$_2$Mo(PyrIm)$_2$ **1** might also be a suitable deposition precursor.

We had previously found ligand-design success by utilizing asymmetric ligands,[15] that combine moieties which contribute to desirable volatilities and thermal stabilities in one ligand. For example, the *tert*-butyl(pyridine-2-yl-methyleneamine adduct of (^{t}BuN)$_2$MoCl$_2$ (**F**), resulted in a volatile and thermally stable compound, where the volatility was conferred from the *tert*-butylimino moiety and the thermal stability from the basic pyridyl ring of the ligand.[15] From this, we speculated that (^{t}BuN)$_2$Mo(PyrIm)$_2$ **1** might also be sufficiently thermally stable due to the presence of the aromatic pyrrolate moiety. Thus, after investigating the volatility of (^{t}BuN)$_2$Mo(PyrIm)$_2$ **1**, its thermal stability was also probed. The thermal stability of **1** was monitored using a "thermal stress test,"[29] where the kinetics of evaporation were exploited (Figure 5). In such experiments, if the precursor decomposes as it volatilizes, increasing the initial mass loading results in a larger residual mass. However, even with a 50 mg mass loading of **1**, only a negligible residual mass (1.8%) was observed. In contrast, (^{t}BuN)$_2$Mo(dpamd)$_2$ (**2**) shows a slight increase to the

residual mass with increased loading (Figure S32). Additionally, there appear to be two thermal processes in the derivative of the mass-loss curve of **2** with higher initial mass loadings. This suggests that **2** initially volatilizes, then undergoes decomposition at higher temperatures, before complete evaporation (Figure S33). These thermal properties make **1** the preferred potential precursor of the two.

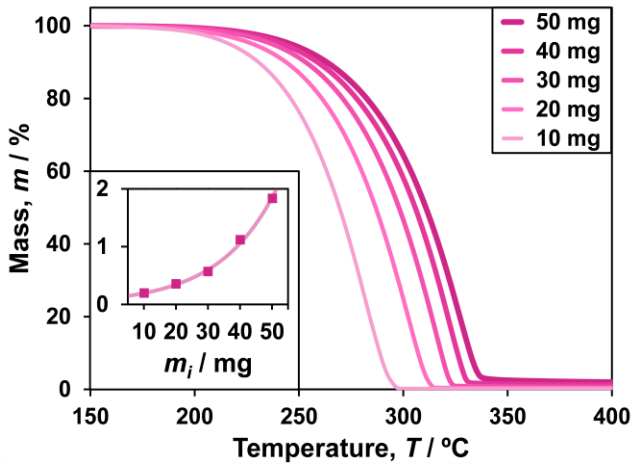

Figure 5. Thermal "stress test" of (^{t}BuN)$_2$Mo(PyrIm)$_2$ (**1**) using TGA. The inset shows the increase in the residual mass (m) with increased initial mass loadings (m_i) highlighting the thermal stability of **1**. The heating rate for all experiments was 10 ºC·min^{-1}.

Differential scanning calorimetry (DSC) was used to further study the thermal properties of (^{t}BuN)$_2$Mo(PyrIm)$_2$ **1**. Inspection of the DSC curve of **1** revealed two endothermic processes, with onset temperatures of 92 and 202 ºC (Figure 6). The first endothermic process is an irreversible phase change with a low enthalpy (ΔH = 2.2 kcal·mol^{-1}); it likely corresponds to ligand rotation, or some other low-barrier, albeit irreversible, geometric isomerization. A C_6D_6 solution of **1** held at 120 ºC for 24 h did not show any changes in its ^{1}H NMR spectrum, suggesting the observed phase change is either limited to the solid state, is reversible *in situ*, or has the same chemical shifts as an unperturbed sample of **1**.

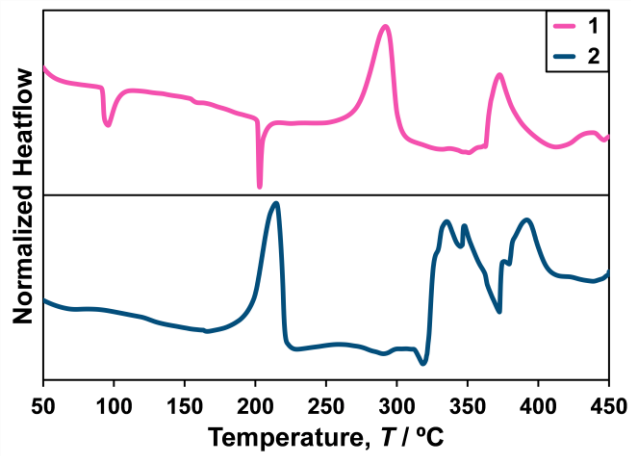

Figure 6. Differential scanning calorimetry plots of (^{t}BuN)$_2$Mo(PyrIm)$_2$ (**1**) (pink, top) and (^{t}BuN)$_2$Mo(dpamd)$_2$ (**2**) (blue, bottom). A heating rates of 10 ºC·min^{-1} was used for both experiments. Exothermic processes correspond to an increase in heat flow (T_D at 273 ºC for **1** and 195 ºC for **2**).

The second endothermic process observed in the DSC curve of **1** (202 ºC) is reversible and corresponds to the melting point of **1**; this was confirmed using an *ex situ* melting point measurement. Following the second endothermic process is a large, irreversible, exothermic process, that begins at 273 ºC, and which has been assigned to the onset of decomposition (T_D) of **1**; thermal events after the initial decomposition of the precursor were not investigated. The thermal range of **1** is quite good ($\Delta T = T_D - T_V$ = 61 ºC), further suggesting it would be a suitable deposition precursor.

(^{t}BuN)$_2$Mo(dpamd)$_2$ **2** was also studied using DSC but it did not melt, and it has a T_D of 195 ºC, which is significantly lower than that of **1**. This is unsurprising since amidinate ligands have several available low-temperature decomposition pathways.[29–32] Many attempts have been made to enhance the thermal stability of amidinates, however, this often comes at the cost of reduced volatility.[29,30] Additionally, the lower T_D of **2** likely explains the theorized decomposition observed in the TGA stress-test of **2.**

It is well known that bis(*tert*-butylimido)molybdenum(VI) adducts decompose to yield isobutylene,[7,10,15,16,33,34] assuming that lower-temperature “ancillary ligand-centered” decompositions do not occur. Therefore, isobutylene was anticipated to be the primary decomposition product in the thermolysis of **1**. To further monitor the thermal stability of

1, and to identify decomposition products, an *in situ* thermolysis reaction was carried out on a C_6D_6 solution of **1** in a flame-sealed NMR tube. The NMR tube was stored in a 200 ºC oven (the highest temperature that can safely, and reliably, be reached for extended periods of time in a sealed tube).

In situ thermolysis was monitored over the course of two months, and **1** appeared to decompose with second-order kinetics, giving a calculated half-life of 23 days at 200 ºC (Figure S14). The observed *in situ* thermolysis products were isobutylene and *tert*-butylamine (as identified by ^{1}H NMR). Both were formed with first-order kinetics and had calculated half-lives of 20 and 21 days, respectively. Additionally, a small amount of the neutral ligand precursor (HPyrIm) was also observed, albeit growing in very slowly, with a calculated half-life of 64 days. Overall, the *in situ* thermolysis at 200 ºC was very slow, further highlighting the excellent thermal stability of **1**.

In contrast to *in situ* thermolysis, solid-state thermolysis more accurately emulates the conditions of a solid-precursor delivery vessel. For example, the *in situ* thermolysis of **1** was carried out in a C_6D_6 solution, whereas solvent is not present in a precursor delivery vessel. Molecular rotations might occur more easily in solution, possibly leading to different product distributions *in situ* than might be achieved for thermolysis *in lieu* of solvent. To probe this, a solid sample of **1** was heated to 300 ºC, under dynamic vacuum. After thermolysis, the mixture was analysed using ^{1}H NMR spectroscopy (after removal of a black residue by filtration). Isobutylene and HPyrIm were observed, however, *tert*-butylamine was not. This suggests that slightly different decomposition mechanisms are operative depending on the thermodynamic conditions (vide infra).

tert-Butylamine is a major decomposition product in the thermolysis of $(^tBuN)_2MoCl_2$ adducts.[16,33] It forms *via* an intramolecular *γ*-H transfer (of a ^{t}BuN proton) to another imido moiety, resulting in a *tert*-butylamido ligand and a nitrido (Mo≡N) moiety.[16] A previous report, based specifically on the thermolysis of $(^tBuN)_2Mo(Pz)$ (**A**),[10] proposed that *γ*-H activation, to yield isobutylene and a hydrogen-terminated imido (Mo=NH), occurs first. It is followed by an intramolecular proton transfer to the pyrazolate, resulting in the elimination of the neutral pyrazole ligand precursor (HPz).[10] We have recently shown that the barrier to Mo=NH formation is quite high (*ca.* 65-70 kcal·mol^{-1}).[16]

Here we speculate that the *γ*-H likely undergoes an intramolecular transfer directly to the pyrrolate ring in **1** (Scheme 2). The crystal structure of **1** contains a short C22a−H22a…N1$_{pyrrole}$ interaction (H22a…N1 = 2.88 Å, Figure 2). Such a transfer would result in the direct formation of isobutylene and HPyrIm, which as a neutral ligand can subsequently dissociate from the metal complex. Alternatively, the *γ*-H could initially undergo intramolecular transfer to the second imido moiety, resulting in a *tert*-butylamido ligand, followed by an intramolecular proton transfer to the pyrrolate ligand. The latter likely occurs in the *in situ* thermolysis where *tert*-butylamine was found to be the most abundant. The *γ*-H elimination of both *tert*-butylimido groups, and the dissociation of both HPyrIm ligands, would result in the formation of metastable "MoN_2". This could subsequently decompose into various molybdenum nitrides, MoN_x (Equations 1-3,[10,35,36] observed here as a solid black residue during the solid-state thermolysis of **1**).[16,33] Therefore, (^{t}BuN)$_2$Mo(PyrIm)$_2$ **1** should make a suitable single-source precursor for the CVD of MoN_x.

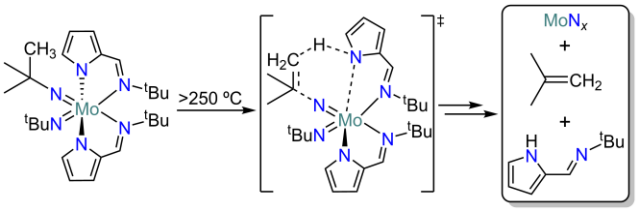

Scheme 2. Proposed solid-state thermal decomposition of (^{t}BuN)$_2$Mo(PyrIm)$_2$ (**1**).

$$2\ MoN_2 \rightarrow 2\ MoN + N_2 \quad (1)$$

$$4\ MoN_2 \rightarrow 2\ Mo_2N + 3\ N_2 \quad (2)$$

$$3\ MoN_2 \rightarrow Mo_3N_2 + 2\ N_2 \quad (3)$$

Conclusion

A bis(*tert*-butylimido)molybdenum(VI) complex incorporating two *N,N'*-κ_2-monoanionic *N*-2-(*tert*-butyliminomethyl)pyrrolato ligands, (^{t}BuN)$_2$Mo(PyrIm)$_2$ (**1**), has been synthesized from a salt metathesis reaction of (^{t}BuN)$_2$MoCl$_2$·dme. This compound has been fully characterized using spectroscopic techniques and both **1** and the neutral ligand precursor have been investigated using single-crystal X-ray crystallography. The

volatility of **1** has been assessed using TGA and it was found to have a vapor pressure of 1 Torr at 212 ºC. It was also found to be sufficiently thermally stable, with a T_D of 273 ºC. Comparisons of **1** to the known vapor deposition precursor, (^{t}BuN)$_2$Mo(dpamd)$_2$ (**2**), revealed them to have similar volatilities, however, **1** showed superior thermal stability. The decomposition of **1** has been investigated using *in situ* and solid-state thermolysis reactions, which revealed isobutylene and either *tert*-butylamine or *N*-2-(*tert*-butyliminomethyl)pyrrole, respectively, as the primary decomposition products. To summarize, **1** exhibits sufficient volatility and has an excellent thermal range (ΔT = 61 ºC) making it a potential vapor deposition precursor, which should be further explored.

Experimental Section

Synthesis. *General Experimental.* All manipulations were performed under air-free conditions using either standard Schlenk techniques or in a nitrogen-filled (99.998% purity) MBraun glovebox. Sodium molybdate (≥98%), triethylamine (≥99%), chlorotrimethylsilane (≥98%), *tert*-butylamine (98%), 1,2-dimethoxyethane (≥99%), and pyrrole-2-carboxaldehyde (98%) were purchased from Sigma-Aldrich and were used as received. Sodium hydride (60% dispersion in mineral oil) was also purchased from Sigma-Aldrich and was washed with hexane prior to use. *N*-2-(*tert*-butyliminomethyl)pyrrole (HPyrIm),[20] (^{t}BuN)$_2$MoCl$_2$·dme,[19,37] and (^{t}BuN)$_2$Mo(dpamd)$_2$ (**2**)[7] were prepared following known methods. All solvents (ACS reagent-grade) were purified using an MBraun Solvent Purification System and were stored over 4 Å molecular sieves. All glassware was oven-dried at 130 ºC, for at least 3 hours, prior to use. ^{1}H, ^{13}C{^{1}H}, and ^{15}N NMR spectra were collected on either a Bruker AVANCE 300 MHz spectrometer or a JEOL RESONANCE ECZ400S (400 MHz) spectrometer, at room temperature. ^{1}H and ^{13}C NMR spectra are internally referenced to residual solvent (^{1}H: δ = 7.16 ppm; ^{13}C: δ = 128.06 ppm for C_6D_6) and ^{15}N spectra are referenced to an external standard of CH_3NO_2 (90% in $CDCl_3$, δ =

380.23 ppm). C_6D_6 was purchased from Cambridge Isotope Laboratories, Inc. and was degassed using freeze-pump-thaw cycles prior to being stored over 4 Å molecular sieves under nitrogen. High-resolution mass spectra were collected on a Kratos Concept electron impact mass spectrometer, at the University of Ottawa. Elemental analysis (EA) was performed on a PerkinElmer 2400 combustion CHN analyser at the University of Windsor.

*Synthesis of (^{t}BuN)$_2$Mo(PyrIm)$_2$ (**1**)*. Solid sodium hydride (0.309 g, 12.9 mmol) was added to a solution of *N*-2-(*tert*-butyliminomethyl)pyrrole (1.642 g, 10.93 mmol) in 100 mL of THF, at room temperature. After the evolution of hydrogen gas had ceased (*ca.* 2 h) a solution of (^{t}BuN)$_2$MoCl$_2$·dme (2.158 g, 5.406 mmol) in 15 mL of toluene was slowly added to the first solution. The mixture was stirred at room temperature for 18 h then the volatiles were removed under reduced pressure. The product was extracted into 60 mL of toluene and filtered through Celite. The volatiles of the filtrate were removed under reduced pressure, resulting in an orange powder. The product was then isolated as red block-shaped crystals after storing a toluene solution at −30 ºC for 48 h. The crystals were subsequently crushed and dried *in vacuo* prior to analysis. Yield = 1.757 g (3.274 mmol, 61%). Mp = 200-201 ºC. ^{1}H NMR (400 MHz, C_6D_6, ppm): *δ* 1.06 (s, 18H, C(C*H*$_3$)$_3$), 1.21 (s, 18H, Mo=NC(C*H*$_3$)$_3$), 6.60 (m, 2H, C(2)*H* of pyrrole), 6.80 (m, 2H, C(3)*H* of pyrrole), 7.33 (m, 2H, C(1)*H* of pyrrole), 7.93 (s, 2H, N=C(5)*H*). ^{13}C{^{1}H} NMR (100 MHz, C_6D_6, ppm): *δ* 30.4 (C(*C*H$_3$)$_3$), 30.9 (Mo=NC(*C*H$_3$)$_3$), 59.4 (*C*(CH$_3$)$_3$), 70.8 (Mo=N*C*(CH$_3$)$_3$), 112.0 (*C*(2)H of pyrrole), 115.5 (*C*(3)H of pyrrole), 139.8 (*C*(4) of pyrrole), 140.6 (*C*(1)H of pyrrole), 153.0 (N=*C*H). ^{15}N NMR (40 MHz C_6D_6, ppm): *δ* 95.7 (Mo=*N*C(CH$_3$)$_3$), 208.0 (*N*=CH), 285.2 (*N*(1) of pyrrole). Selected IR data (KBr, cm^{-1}): *ν*(Mo=N) 1203 (vs) &

1225(s); *v*(N=C) 1603 (vs). EA calcd for $C_{26}H_{44}MoN_6$ [%]: C, 58.19; H, 8.26; N, 15.66; found [%]: C, 57.75; H, 7.87; N, 15.46. HRMS (EI) *m/z*: $[M]^+$ calcd for $C_{25}H_{41}MoN_6$ 538.2682; Found 538.2682.

Thermal Characterization. *Thermogravimetric Analysis.* TGA was performed on a TA Instruments Discovery TGA 55 instrument which was housed in a "chemical-free", nitrogen-filled (99.998%) MBraun Labmaster 130 glovebox. In a typical experiment 10.000 ± 0.100 mg of analyte was placed in a platinum pan and heated to 500 ºC with a ramp rate of 10 ºC min^{-1}, unless otherwise stated, using nitrogen (99.999% purity, 60 sccm) as the purge gas. Platinum pans were cleaned by sequential sonication in glacial acetic acid then isopropanol, followed by heating until red-hot with a propane torch. Langmuir vapor pressure equations were derived from the TGA data using a previously reported method, employing benzoic acid as the calibrant.[27,28]

Differential Scanning Calorimetry. DSC experiments were performed with a TA Instruments Q10 instrument. The DSC was calibrated at the melting point of indium metal (156.6 ºC). All DSC samples were hermetically sealed in aluminum pans inside a glovebox prior to analysis. All samples were heated to 500 ºC with a ramp rate of 10 ºC min^{-1}, unless otherwise stated, using nitrogen (99.998% purity, 50 sccm) as the purge gas.

*Solid-State Thermolysis of **1**.* The solid compound (0.120 g of **1**) was weighed into a 25 mL Schlenk flask and placed under static vacuum (40 mTorr). The flask was then slowly, and thoroughly, heated with a heat-gun (~300 ºC). The compound gradually darkened, eventually forming a blackish-brown residue and a metallic-like film on the inside of the flask (Figure S8). After the thermolysis, the flask was slowly cooled to room

temperature then 2 mL of C_6D_6 was added to the flask, under nitrogen. The mixture was filtered through a pad of Celite, directly into an NMR tube, giving a brownish-orange solution. ^{1}H NMR spectroscopy revealed signals assigned to the intact precursor (**1**), as well as isobutylene and *N*-2-(*tert*-butyliminomethyl)pyrrole (Figure S9).

*In Situ Thermolysis of **1**.* (^{t}BuN)$_2$Mo(PyrIm)$_2$ **1** was dissolved in C_6D_6, in a thick-walled NMR tube. The solution was frozen in liquid nitrogen and the NMR tube was flame-sealed under vacuum. It was stored at room temperature for 18 hours to ensure stoichiometry and stability. The flame-sealed NMR tube was then placed in an oven with an internal temperature of 200 ºC and left for two months. ^{1}H NMR spectra were collected every few days, to show stability, and identify the thermolysis products (Figure S11).

X-Ray Crystallography. The crystallographic diagrams in the main manuscript were prepared using ORTEP-3 for Windows.[38] Specific details about the data collections and refinements can be found in the Supporting Information.

Supporting Information

NMR, IR and HRMS spectra; TGA plots; DSC curves; crystallographic information files for all compounds deposited at the CCDC (2201553-2201556) (PDF).

Author Information

Corresponding Author

*E-mail: Michael.land@carleton.ca

ORCID

Michael A. Land: 0000-0001-5861-242X

Dexter A. Dimova: 0000-0003-0182-3407

Katherine N. Robertson: 0000-0002-5602-8059

Seán T. Barry: 0000-0001-5515-4734

Author Contributions

The manuscript was written through contributions of all authors. All authors have given approval to the final version of the manuscript.

Acknowledgements

M.A.L. thanks the Natural Sciences and Engineering Council of Canada (NSERC) for funding through the Alexander Graham Bell CGS-D Scholarship. S.T.B. acknowledges NSERC for support through the Discovery Grants Program (RGPIN-2019-06213). We also thank Sharon Curtis, from the University of Ottawa, for HRMS acquisition and Lara Watanabe, from the University of Windsor, for EA acquisition.

References

(1) He, Y.; Feng, J. Y. Diffusion Barrier Performances of Direct Current Sputter-Deposited Mo and MoxN Films between Cu and Si. *Journal of Crystal Growth* **2004**, *263* (1–4), 203–207. https://doi.org/10.1016/j.jcrysgro.2003.11.005.

(2) Führer, M.; Van Haasterecht, T.; Bitter, J. H. Molybdenum and Tungsten Carbides Can Shine Too. *Catalysis Science and Technology* **2020**, *10* (18), 6089–6097. https://doi.org/10.1039/d0cy01420f.

(3) Mattinen, M.; Wree, J.-L.; Stegmann, N.; Ciftyurek, E.; Achhab, M. El; King, P. J.; Mizohata, K.; Räisänen, J.; Schierbaum, K. D.; Devi, A.; Ritala, M.; Leskelä, M. Atomic Layer Deposition of Molybdenum and Tungsten Oxide Thin Films Using Heteroleptic Imido-Amidinato Precursors: Process Development, Film Characterization, and Gas Sensing Properties. *Chemistry of Materials* **2018**, *30* (23), 8690–8701. https://doi.org/10.1021/acs.chemmater.8b04129.

(4) Splendiani, A.; Sun, L.; Zhang, Y.; Li, T.; Kim, J.; Chim, C. Y.; Galli, G.; Wang, F. Emerging Photoluminescence in Monolayer MoS2. *Nano Letters* **2010**, *10* (4), 1271–1275. https://doi.org/10.1021/nl903868w.

(5) Spalvins, T. A Review of Recent Advances in Solid Film Lubrication. *Journal of Vacuum Science & Technology A: Vacuum, Surfaces, and Films* **1987**, *5* (2), 212–219. https://doi.org/10.1116/1.574106.

(6) Barry, S. T. Amidinates, Guanidinates and Iminopyrrolidinates: Understanding Precursor Thermolysis to Design a Better Ligand. *Coordination Chemistry Reviews* **2013**, *257* (23–24), 3192–3201. https://doi.org/10.1016/j.ccr.2013.03.015.

(7) Gwildies, V.; Thiede, T. B.; Amirjalayer, S.; Alsamman, L.; Devi, A.; Fischer, R. A. All-Nitrogen Coordinated Amidinato/Imido Complexes of Molybdenum and Tungsten: Syntheses and Characterization. *Inorganic Chemistry* **2010**, *49* (18), 8487–8494. https://doi.org/10.1021/ic101060s.

(8) Srinivasan, N. B.; Thiede, T. B.; de los Arcos, T.; Gwildies, V.; Krasnopolski, M.; Becker, H. W.; Rogalla, D.; Devi, A.; Fischer, R. A. Transition Metal Nitride Thin Films Grown by MOCVD Using Amidinato Based Complexes [M(NtBu)2{(IPrN)2CMe}2] (M=Mo, W) as Precursors. *Surface and Coatings Technology* **2013**, *230*, 130–136. https://doi.org/10.1016/j.surfcoat.2013.06.024.

(9) Cwik, S.; Mitoraj, D.; Mendoza Reyes, O.; Rogalla, D.; Peeters, D.; Kim, J.; Schütz, H. M.; Bock, C.; Beranek, R.; Devi, A. Direct Growth of MoS2 and WS2 Layers by Metal Organic Chemical Vapor Deposition. *Advanced Materials Interfaces* **2018**, *5* (16), 1–11. https://doi.org/10.1002/admi.201800140.

(10) Dezelah IV, C. L.; El-Kadri, O. M.; Heeg, M. J.; Winter, C. H. Preparation and Characterization of Molybdenum and Tungsten Nitride Nanoparticles Obtained by Thermolysis of Molecular Precursors. *Journal of Materials Chemistry* **2004**, *14* (21), 3167–3176. https://doi.org/10.1039/b405636a.

(11) Wree, J. L.; Ciftyurek, E.; Zanders, D.; Boysen, N.; Kostka, A.; Rogalla, D.; Kasischke, M.; Ostendorf, A.; Schierbaum, K.; Devi, A. A New Metalorganic Chemical Vapor Deposition Process for MoS2with a 1,4-Diazabutadienyl Stabilized Molybdenum Precursor and Elemental Sulfur. *Dalton Transactions* **2020**, *49* (38), 13462–13474. https://doi.org/10.1039/d0dt02471f.

(12) Rische, D. MOCVD of Tungsten and Molybdenum Nitrides, 2007.

(13) Park, G.; Cho, Y.; Sato, H.; Harano, K.; Uchiuzou, H. Molybdenum Compound and Method of Manufacturing Integrated Circuit Device Using the Same. US 2021/0300955A1, 2021.

(14) Gaess, D.; Harms, K.; Pokoj, M.; Stolz, W.; Sundermeyer, J. Volatile Imido−Hydrazido Compounds of the Refractory Metals Niobium, Tantalum, Molybdenum, and Tungsten. *Inorganic Chemistry* **2007**, *46* (16), 6688–6701. https://doi.org/10.1021/ic062435e.

(15) Land, M. A.; Bačić, G.; Robertson, K. N.; Barry, S. T. Thermal Stability and Decomposition Pathways in Volatile Molybdenum(VI) Bis-Imides. *Inorganic Chemistry* **2022**, *61* (12), 4980–4994. https://doi.org/10.1021/acs.inorgchem.1c03817.

(16) Land, M. A.; Bačić, G.; Robertson, K. N.; Barry, S. T. The Origin of Decomposition in a Family of Influential Molybdenum Precursor Compounds. No. Vi, 1–58.

(17) Chiu, H.-T.; Chang, G.-B.; Ho, W.-Y.; Chuang, S.-H.; Lee, G.-H.; Peng, S.-M. Syntheses and X-Ray Crystal Structures of Dichlorobis(Tert-Butylimido) Complexes of Molybdenum(VI); Potential Precursors to Molybdenum Nitride and Molybdenum Carbonitride. *Journal of the Chinese Chemical Society* **1994**, *41* (6), 755–761. https://doi.org/10.1002/jccs.199400106.

(18) Zanders, D.; Liu, J.; Obenlüneschloß, J.; Bock, C.; Rogalla, D.; Mai, L.; Nolan, M.; Barry, S. T.; Devi, A. Cobalt Metal ALD: Understanding the Mechanism and Role of Zinc Alkyl Precursors as Reductants for Low-Resistivity Co Thin Films. *Chemistry of Materials* **2021**, *33* (13), 5045–5057. https://doi.org/10.1021/acs.chemmater.1c00877.

(19) Fox, H. H.; Yap, K. B.; Robbins, J.; Cai, S.; Schrock, R. R. Simple-High Yield Syntheses of Molybdenum(VI) Bis(IMIDO) Complexes of the Type Mo(NR)2Cl2(1, 2-Dimethoxyethane). *Inorganic Chemistry* **1992**, *31* (11), 2287–2289. https://doi.org/10.1021/ic00037a056.

(20) Grushin, V.; Marshall, W. Water as an Ideal Solvent for the Synthesis of Easily Hydrolyzable Compounds: High-Yield Preparation of 2-Pyrrolecarbaldimines and Their CVD/ALD-Relevant Cu(II) Derivatives in H2O. *Advanced Synthesis & Catalysis* **2004**, *346* (12), 1457–1460. https://doi.org/10.1002/adsc.200404181.

(21) Baltrun, M.; Watt, F. A.; Schoch, R.; Hohloch, S. Dioxo-, Oxo-Imido-, and Bis-Imido-Molybdenum(VI) Complexes with a Bis-Phenolate-NHC Ligand. *Organometallics* **2019**, *38* (19), 3719–3729. https://doi.org/10.1021/acs.organomet.9b00472.

(22) Hüttinger, K.; Förster, C.; Bund, T.; Hinderberger, D.; Heinze, K. Stereochemical Consequences of Oxygen Atom Transfer and Electron Transfer in Imido/Oxido Molybdenum(IV, V, VI) Complexes with Two Unsymmetric Bidentate Ligands. *Inorganic Chemistry* **2012**, *51* (7), 4180–4192. https://doi.org/10.1021/ic202588u.

(23) Stalzer, M. M.; Lohr, T. L.; Marks, T. J. Synthesis, Characterization, and Thermal Properties of N -Alkyl β-Diketiminate Manganese Complexes. *Inorganic Chemistry* **2018**, *57* (6), 3017–3024. https://doi.org/10.1021/acs.inorgchem.7b02476.

(24) Thiede, T.; Gwildies, V.; Alsamann, L.; Rische, D.; Fischer, R. Novel Precursors for the MOCVD of Molybdenum Nitride. In *ECS Transactions*; ECS, 2009; Vol. 25, pp 593–600. https://doi.org/10.1149/1.3207645.

(25) Groom, C. R.; Bruno, I. J.; Lightfoot, M. P.; Ward, S. C. The Cambridge Structural Database. *Acta Crystallographica Section B Structural Science, Crystal Engineering and Materials* **2016**, *72* (2), 171–179. https://doi.org/10.1107/S2052520616003954.

(26) El-Kadri, O. M.; Heeg, M. J.; Winter, C. H. Film Growth Precursor Development for Metal Nitrides. Synthesis, Structure, and Volatility of Molybdenum(vi) and Tungsten(vi) Complexes Containing Bis(Imido)Metal Fragments and Various Nitrogen Donor Ligands. *Dalton Transactions* **2006**, No. 16, 1943–1953. https://doi.org/10.1039/b515378f.

(27) Price, D. M. Vapor Pressure Determination by Thermogravimetry. *Thermochimica Acta* **2001**, *367–368* (June 2000), 253–262. https://doi.org/10.1016/S0040-6031(00)00676-6.

(28) Price, D. M. A Fit of the Vapours. *Thermochimica Acta* **2015**, *622*, 44–50. https://doi.org/10.1016/j.tca.2015.04.030.

(29) Coyle, J. P.; Kurek, A.; Pallister, P. J.; Sirianni, E. R.; Yap, G. P. A.; Barry, S. T. Preventing Thermolysis: Precursor Design for Volatile Copper Compounds. *Chemical Communications* **2012**, *48* (84), 10440. https://doi.org/10.1039/c2cc35415b.

(30) Beh, E. S.; Tong, L.; Gordon, R. G. Synthesis of 5,5-Bicyclic Amidines as Ligands for Thermally Stable Vapor Deposition Precursors. *Organometallics* **2017**, *36* (8), 1453–1456. https://doi.org/10.1021/acs.organomet.6b00954.

(31) Barry, S. T. Amidinates, Guanidinates and Iminopyrrolidinates: Understanding Precursor Thermolysis to Design a Better Ligand. *Coordination Chemistry Reviews* **2013**, *257* (23–24), 3192–3201. https://doi.org/10.1016/j.ccr.2013.03.015.

(32) Wu, J.; Li, J.; Zhou, C.; Lei, X.; Gaffney, T.; Norman, J. A. T.; Li, Z.; Gordon, R.; Cheng, H. Computational Study on the Relative Reactivities of Cobalt and Nickel Amidinates via β-H Migration. *Organometallics* **2007**, *26* (11), 2803–2805. https://doi.org/10.1021/om060910a.

(33) Land, M. A.; Robertson, K. N.; Barry, S. T. Ligand-Assisted Volatilization and Thermal Stability of Bis(Imido)Dichloromolybdenum(VI) ([(t-BuN═)2MoCl2]2) and Its Adducts. *Organometallics* **2020**, *39* (7), 916–927. https://doi.org/10.1021/acs.organomet.9b00578.

(34) Ou, N. C.; Preradovic, K.; Ferenczy, E. T.; Sparrow, C. B.; Germaine, I. M.; Jurca, T.; Craciun, V.; Mcelwee-White, L. Synthesis and Evaluation of Molybdenum Imido-Thiolato Complexes for the Aerosol-Assisted Chemical Vapor Deposition of Nitrogen-Doped Molybdenum Disulfide. *Organometallics* **2020**, *39* (7), 956–966. https://doi.org/10.1021/acs.organomet.9b00705.

(35) Yu, S.; Huang, B.; Jia, X.; Zeng, Q.; Oganov, A. R.; Zhang, L.; Frapper, G. Exploring the Real Ground-State Structures of Molybdenum Dinitride. *The Journal of Physical Chemistry C* **2016**, *120* (20), 11060–11067. https://doi.org/10.1021/acs.jpcc.6b00665.

(36) Sun, W.; Holder, A.; Orvañanos, B.; Arca, E.; Zakutayev, A.; Lany, S.; Ceder, G. Thermodynamic Routes to Novel Metastable Nitrogen-Rich Nitrides. *Chemistry of Materials* **2017**, *29* (16), 6936–6946. https://doi.org/10.1021/acs.chemmater.7b02399.

(37) Dyer, P. W.; Gibson, V. C.; Howard, J. A. K.; Whittle, B.; Wilson, C. Four Coordinate Bis(Imido) Alkene Complexes of Molybdenum(IV): Relatives of the Zirconocene Family. *Journal of the Chemical Society, Chemical Communications* **1992**, *04* (22), 1666–1668. https://doi.org/10.1039/C39920001666.

(38) Farrugia, L. J. WinGX and ORTEP for Windows : An Update. *Journal of Applied Crystallography* **2012**, *45* (4), 849–854. https://doi.org/10.1107/S0021889812029111.

For Table of Contents Only

A new thermally robust bis(*tert*-butylimido)molybdenum(VI) complex that incorporates two *N,N'*-κ_2-monoanionic ligands was prepared. The compound is volatile and very thermally stable, due incorpoartion of an unsymmetric ligand that combines both properties. Comparisons to a structurally similar deposition precursor show the new compound is superior and should be investigated for use as a deposition precursor.